Understanding Poor Seismic Performance of Concrete Walls and Design Implications

Sri Sritharan,[a] M.EERI, Katrin Beyer,[b] M.EERI, Richard S. Henry[c], Y. H. Chai,[d], Mervyn Kowalsky,[e] M.EERI, and Desmond Bull,[f]

The 2010/2011 Canterbury earthquakes in New Zealand revealed: 1) Improved structural response resulting from historical design advancements; 2) Poor structural performance due to previously identified shortcomings being insufficiently addressed in design practice; and (3) New deficiencies that were not previously recognized because of premature failure resulting from other design flaws. This paper summarizes damage to concrete walls observed in the February 2011 Christchurch earthquake, proposes links between the observed response and specific design concerns, and offers suggestions for improving seismic design of walls in the following areas: amount of longitudinal reinforcement in wall end regions, suitable wall thickness to minimize the potential for out-of-plane buckling, and minimum vertical reinforcement requirements.

INTRODUCTION

Field observations of structural performance in previous earthquakes have significantly contributed to research advancements. Subsequently, improved design procedures and detailing have been adopted in newer structures built in seismic regions around the world. As with the 2010/2011 Canterbury earthquakes in New Zealand, field observations have confirmed the improved seismic performance of structures resulting from historical design advancements. For example, due to the stringent application of the capacity design approach, classical shear failures of reinforced concrete walls were rare. However, new or previously uncommon failure modes were observed to reinforced concrete walls especially in the 2011 Christchurch earthquake. This paper focuses on the performance of reinforced concrete walls

[a] Iowa State University, Ames, IA 50010, USA
[b] École Polytechnique Fédérale de Lausanne (EPFL), 1015 Lausanne, Switzerland
[c] University of Auckland, Auckland 1142, New Zealand
[d] University of California, Davis, CA 95616, USA
[e] North Carolina State University Raleigh, NC 27695, USA
[f] Holmes Consulting Group and University of Canterbury, Christchurch 8140, New Zealand

in the 2011 Christchurch earthquake, where ductile design details were adopted, but the expected flexural hinge did not form.

Using results of experimental and analytical research, this paper draws attention to some critical design issues and provides suggestions for improving reinforced concrete wall performance in future earthquakes. With emphasis on achieving ductile behavior for reinforced concrete walls, this paper specifically addresses: (a) Impact of concentrating the main longitudinal (i.e., vertical) reinforcement in wall boundary elements instead of distributing it along the wall length; (b) Influence of large tensile strain demand on the longitudinal reinforcement causing local buckling of the wall due to compression zone instability upon subsequent load reversal; and (c) Consequence of not providing adequate minimum vertical reinforcement in walls.

DESIGN PRACTICE

CURRENT APROACH

In modern seismic design, reinforced concrete walls are designed with the intention of providing sufficient strength and adequate flexural ductility while preventing brittle failure modes such as those from insufficient shear capacity, inadequate anchorage of reinforcement, inadequate lap splice length, and sliding at the wall-to-foundation interface. While some design standards aim to achieve ductile wall response by adopting the capacity design philosophy (e.g., NZ 3101:2006; CEN 2004), others attempt to achieve the same behavior without explicitly implementing this design philosophy (e.g., ACI 318-11).

A common feature of seismic force-resisting walls subjected to large moments and shears is that they are designed with boundary elements, which are regions located at the wall ends with additional reinforcement requirements, increased thickness or both. Comparable to highly reinforced ductile columns, these regions may use a combination of high concentration of longitudinal and transverse reinforcement to ensure that high compressive strains needed for ductile wall response can be developed in these regions. This is why ACI 318 (2011) and Eurocode 8 (CEN 2004) require the use of boundary elements in walls when compression in the wall's end regions exceeds certain stress or strain limits. Although confinement reinforcement is required in the compression zone, the NZS 3101 (2006) standards do not require the use of boundary elements, but encourages it by allowing slightly larger curvature ductility demand to be developed in the plastic hinge regions of walls with

boundary elements. In this case, there is no specific requirement to use a concentration of longitudinal reinforcement, because it aims at minimizing the likelihood of the wall experiencing out-of-plane buckling as subsequently discussed. Though not required, one reason for using larger diameter longitudinal bars in the end regions is to increase the minimum required spacing of transverse reinforcement, reducing the steel congestion. Another benefit of the highly reinforced boundary elements is that it increases the moment resistance of the walls by 5-15% compared to walls with the same total area of longitudinal reinforcement distributed evenly along the wall length (Dai 2012). In these situations, the wall regions between the boundary elements are typically designed with minimum amounts of vertical reinforcement in two parallel layers.

To limit premature out-of-plane buckling of walls in the potential plastic hinge region, NZS 3101 controls the minimum wall thickness as a function of wall length and aspect ratio. While the commentary section of NZS 3101 acknowledges that the maximum tensile strain developed in the longitudinal reinforcement influences this wall instability by acknowledging that the original equations proposed by Paulay and Priestley (1992) were used in deriving a simple design equation, the wall thickness is not determined as a function of an expected tensile strain. Eurocode and ACI have requirements for minimum thickness for boundary elements, but they are not based on minimizing potential wall buckling resulting from large tensile strain in the longitudinal reinforcement.

Historically, the minimum vertical reinforcement in concrete walls was based solely on requirements for temperature and shrinkage. Current versions of NZS 3101 and ACI 318 include more rigorous minimum vertical reinforcement limits to ensure that a minimum level of ductility is achieved. NZS 3101 (2006) adopted the same equation for walls as that previously developed for minimum longitudinal reinforcement in beams to ensure that the yield moment is greater than the probable cracking moment. The NZS 3101 (2006) procedure results in vertical reinforcement contents of 0.25% or greater depending on the concrete and reinforcement strength. In special structural walls, ACI 318 requires a minimum reinforcement content of 0.25% that is not dependent on the concrete or reinforcement strength; this can be reduced to 0.12-0.15% when the shear demand is below certain limits. Eurocode 8 requires a minimum vertical reinforcement of 0.25% across cold joints, which is to minimize shear sliding at the crack interface.

POTENTIAL UNDESIRABLE FAILURE MODES

While wall failure resulting from some deficiencies such as insufficient horizontal reinforcement is obvious and have been repeatedly witnessed in past earthquake damage, consequences of some others such as small wall thicknesses that can cause buckling may not be easily identifiable. This is because their impact is difficult to quantify even with the current analysis capabilities. Furthermore, when a wall has been designed with multiple deficiencies, the cause of failure is dominated by the weakest design detail. Before sound ductile design principles were implemented, inadequate confinement and/or shear reinforcement dominated wall failure. In that case, it would have been easier to overlook other deficiencies in the wall. When walls are designed with adequate confinement and shear reinforcement, some of the less obvious design deficiencies will surface, which was observed to a certain degree in Christchurch and formed the basis for this paper.

Distributed vs. Concentrated Longitudinal Reinforcement

Despite the expected benefits and the code recommendations to use heavy longitudinal reinforcement in boundary elements, seismic testing on concrete walls designed with boundary elements has often produced unsatisfactory overall performance at moderate to large ductilities. While the boundary elements exhibit satisfactory response, the web region between the boundary elements experiences significant damage. **Figure 1** shows a rectangular wall, RWN, tested by Aaleti et al. (2013) and a U-shaped concrete wall, TUB, tested by Beyer et al. (2008). The unsymmetrical damage pattern seen on RWN is a reflection of the use of different amounts of vertical reinforcement in the two boundary elements and asymmetric loading to achieve specific research objectives, while TUB was subjected to a bidirectional loading pattern comprising cycles in the web, flange and diagonal directions.

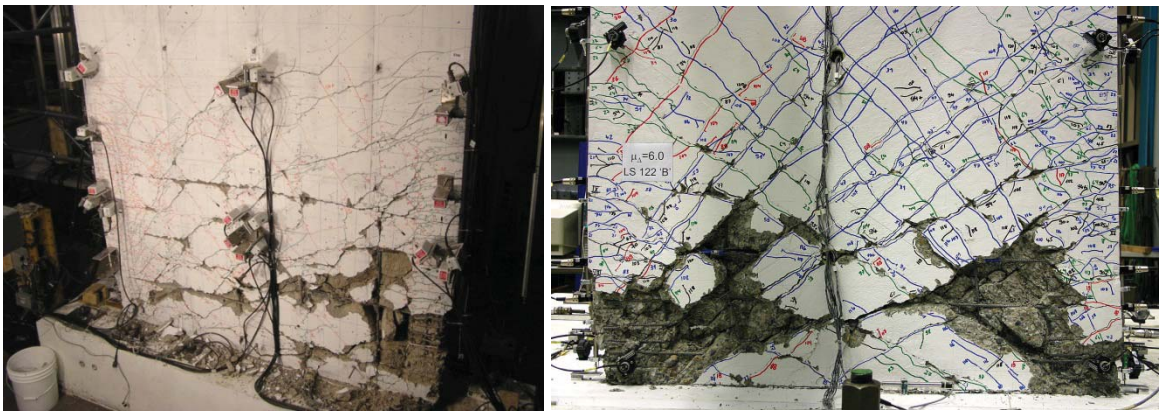

(a) RWN tested by Aaleti et al. (2013) (b) TUB tested by Beyer et al. (2008)

Figure 1 Cyclic testing of concrete walls with boundary elements

An important observation from the two tests is that the extent of damage to walls in the boundary elements is relatively less compared to the web regions. Formation of cracks with larger width and wider spacing, crushing and spalling of concrete that began within the cover and penetrated well into the core region, and subsequent reduction of wall thickness beyond that experienced by the boundary elements are direct consequences of using light reinforcement in the web regions. As evidenced from the tests, potential failure modes of walls with heavy longitudinal reinforcement in the boundary elements and light longitudinal reinforcement in the web regions are: (1) Crushing of concrete in the web regions, which can be exacerbated if the axial load in the walls increases due to vertical acceleration and/or framing action resulting from interaction between walls and floors; and (2) Large shear deformation and potential for shear sliding due to the development of wider cracks in the web; and (3) Buckling of boundary elements due to the web experiencing significant damage. Though the aforementioned web crushing occurs under in-plane loading, Paulay and Priestley (1992) noted that out-of-plane response can also increase the possibility of web crushing especially when low amounts of reinforcement presents in the web region.

Paulay and Priestley (1992) suggested the use of smaller diameter bars with a smaller spacing in the web region as a possibility for improving wall performance based on the tests completed by Iliya and Bertero (1980). Other potential improvements to wall performance have been recently investigated by Brueggen (2009) and Dai (2012). In a T-wall tested by Brueggen, the web of the tee wall was designed following the current ACI practice, including a boundary element. A longer length for the confinement region was used because this was found to be necessary based on a section analysis and noticeable damage observed to this region in NTW1—a reference wall tested by Brueggen (2009) following the code approach. However, the flange of the second wall, NTW2, was designed with distributed reinforcement. This resulted in a longitudinal steel ratio, ρ_l, of 2.16% along the entire length of the flange in NTW2, whereas ρ_l of 3.78% and 0.59% were used, respectively, within and outside of the boundary elements in the flange of NTW1. While the performance of the web in NTW2 improved due to the use of a longer confinement region, the drastic difference to the damage between the boundary element and the region in between the boundary is seen in **Figure 2**a. On the other hand, a significantly improved performance was obtained for the flange with distributed reinforcement (see **Figure 2**b). The distribution of reinforcement in NTW2 resulted in a 13% reduction in lateral force resistance and an increased displacement of 22%

at the maximum lateral load resistance.

Using a systematic analysis, Dai (2012) examined the ductility capacity and failure strains of rectangular concrete walls with distribution of vertical reinforcement as a main variable. This study concluded that improved lateral wall performance may be achieved by distributing at least a portion of the required longitudinal reinforcement along the wall length with appropriate confinement reinforcement in the end regions. In comparison to the ACI 318 (2011) recommendations, the study concluded that overall seismic performance of the walls could be enhanced by increasing the confinement reinforcement quantity by 30% and providing it along the length of the compression regions experiencing strain beyond 0.0015.

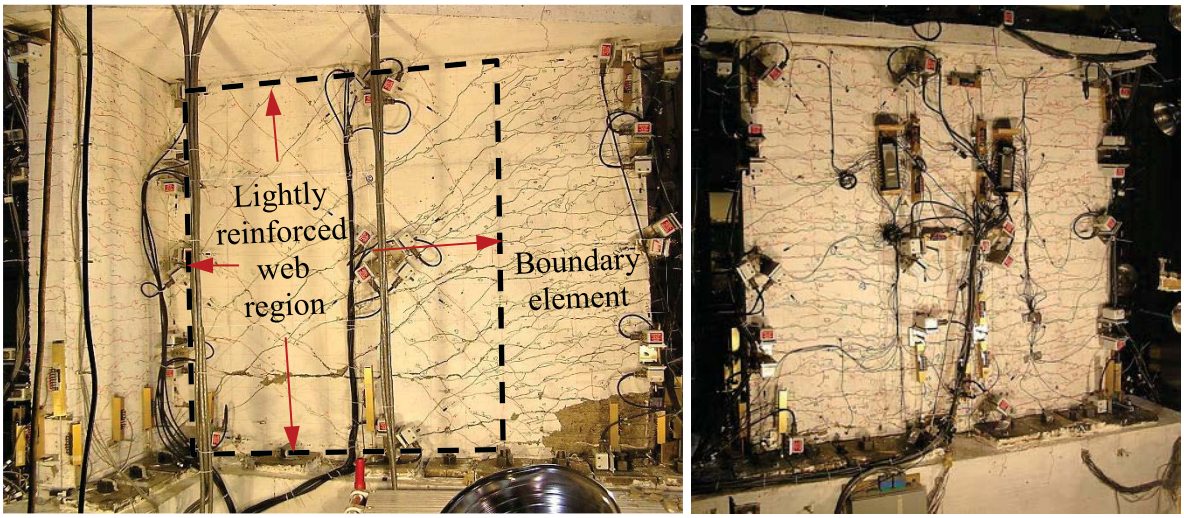

(a) Crack pattern on the web of NTW2 (b) Crack pattern on the back side of flange of NTW2 after web failure

Figure 2 A T-wall test completed by Brueggen with distributed reinforcement in the flange

Instability of Structural Walls

Structural walls designed to current practice can experience significant ductility demand with large tensile strains being imposed on the longitudinal reinforcement in the plastic hinge region. This strain magnitude will depend on the axial load, and importantly, the wall geometry. Concrete and steel properties also impact tensile strain demand, but to a lesser extent. For planar rectangular walls, equilibrium of internal forces dictates the distance to the neutral axis, as measured from the extreme compression fiber, to be greater than that of T, L or U-shaped walls, indicating that for the same curvature the tensile strain in the end region of the wall is higher in the case of non-planar walls. The large tensile strain is of importance as it affects the lateral stability of the wall depending on its magnitude. Cracks, developed as a result of a large inelastic excursion, must close in order to provide the local compressive force needed for

developing the in-plane lateral strength in the reversed direction. The phenomenon, referred to as local wall instability, was first investigated by Goodsir et al. (1983) and Goodsir (1985), and a set of expressions to control wall buckling, as previously noted, was proposed by Paulay and Priestley (1992).

Chai and Elayer (1999) demonstrated the mechanism of wall instability using cyclic tests of axially loaded reinforced concrete columns, which essentially represented the end tension/compression region of walls. Despite the lack of strain gradient effects, such idealization was useful in identifying the critical parameters governing the buckling mechanism. Photographs in **Figure 3** show the condition of a reinforced concrete column under large tension/compression cycles. The test column was rectangular in cross-section (102 mm × 204 mm) and longitudinally reinforced with 6#3 bars (d_b = 9.5 mm, where d_b is the bar diameter) giving a reinforcement ratio of 2.1%. The length of the column was 1498 mm giving a length-to-width ratio of 14.75. Transverse ties were provided at a close spacing of $6d_b$ to represent a well-confined end region of the wall and to prevent local buckling of the longitudinal reinforcement as typically used in design of ductile walls.

The loading protocol for the test column imposed first a tensile half-cycle followed by a compression half-cycle with a compressive strain targeting about 1/7 of the tensile strain amplitude. In **Figure 3**a and b, amplitudes of the axial strain in the tensile half-cycle were 0.0078, 0.0108, 0.0133 and 0.0161. For axial tensile strains less than or equal to 0.0133, the test column was stable and it was able to fully develop the compressive force associated with the target compressive strain and the out-of-plane displacement was small. For a large axial tensile strain of 0.0161, however, significant out-of-plane displacement developed in the compression half-cycle, leading to column buckling. The stable column response following a tensile strain of 0.0133 can be seen in **Figure 3**a, while the buckled column after a tensile strain of 0.0161 is shown in **Figure 3**b. Thus, the tensile strain amplitude must be recognized as an important parameter governing the cyclic stability of reinforced concrete structural walls.

Guided by experimental observations, Chai and Elayer (1999) proposed a phenomenological model for limiting the axial tensile strain in the wall end region to prevent buckling when subjected to reverse cyclic loading. To that end, the critical tensile strain is:

$$\epsilon_{sm} \leq \frac{\pi^2}{2}\left(\frac{b}{l_o}\right)^2 \xi_c + 3\,\epsilon_y \tag{1}$$

where b is the wall thickness, l_o is the buckled length of the wall, which may be taken to be equal to the plastic hinge length of the wall, as recommended by Paulay and Priestley (1993),

and ϵ_y is the yield strain of the reinforcement. The value of $\xi_c$can be found as proposed by Paulay and Priestley (1993) from Eqs. 2 and 3:

$$\xi_c = 0.5\left(1 + 2.35\, m - \sqrt{5.53\, m^2 + 4.70\, m}\right) \tag{2}$$

where m is the mechanical reinforcement ratio, which is defined as

$$m = \rho_{end}\frac{f_y}{f_c'} \tag{3}$$

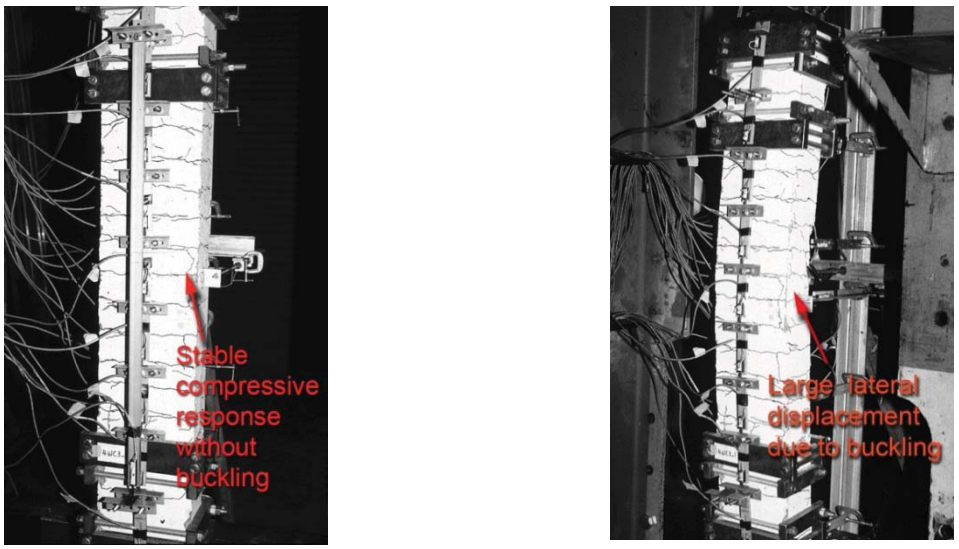

(a) Stable compressive response up to $\epsilon_a = -0.0133$

(b) Unstable compressive response after $\epsilon_a = -0.0161$

Figure 3 Stability of a reinforced concrete column under tensile/compression cycles (Note: negative sign indicates tensile strains)

and ρ_{end} is the local reinforcement ratio appropriate for the end region of the wall, f_y is the yield strength of the longitudinal reinforcement, and f_c' is the uniaxial compressive strength of the concrete. It should be noted that Eq. 4 was proposed earlier by Paulay and Priestley (1993) for the critical tensile strain, which is more conservative than Eq. 1 especially when $\epsilon_{sm} < 0.02$.

$$\epsilon_{sm} \leq 8\beta\left(\frac{b}{l_o}\right)^2 \xi_c \tag{4}$$

where β is a parameter defining the location of the longitudinal reinforcement, which is defined as $\beta = d/b$, where d is the effective depth of the reinforcement. Implications of the critical strain ϵ_{sm} given by Eqs. 1 and 4 are further examined later in the paper.

Minimum Reinforcement Requirement

As required for other flexural members, structural walls must also be designed with a minimum longitudinal reinforcement. When the minimum reinforcement governs the design,

walls are detailed with distributed longitudinal reinforcement along the length and without boundary elements. This issue becomes critical in regions of low to moderate seismicity, such as Christchurch, where the abundance of load-bearing concrete walls in certain building types can result in sufficient lateral resistance being achieved through a combination of axial load effects and minimum vertical reinforcement. As highlighted by Paulay and Priestley (1992), in addition to satisfying the temperature and shrinkage requirements, this minimum vertical reinforcement should ensure a ductile response for the walls. During seismic loading, lightly reinforced concrete walls are vulnerable to sudden failure resulting from fracture of vertical tension reinforcement following the initiation of the first flexural crack and the concentration of inelastic demand largely at this crack as opposed to distributed cracks. Insufficient vertical reinforcement was attributed to failure of several walls during the 1985 Chilean earthquake (Wood et al. 1991). After analyzing the results of 37 wall tests, Wood (1989) concluded that walls with less than 1% longitudinal reinforcement ratio were susceptible to fracture of reinforcing steel. To date the majority of lightly reinforced walls that have been tested are squat walls (Greifenhagen and Lestuzzi 2005; Hidalgo et al. 2002; Wood 1989), which provide limited knowledge for understanding the behavior of flexural dominant walls with minimum vertical reinforcement.

The minimum required vertical reinforcement in walls has historically been less than the equivalent minimum longitudinal reinforcement in beams. Prior to 2006, the New Zealand Concrete Structures Standard required that walls contain a vertical reinforcement ratio greater than of $0.7/f_y$ to account for temperature and shrinkage effects, where f_y is the yield strength of the longitudinal reinforcement in MPa. This equated to ρ_l in the range of 0.14 – 0.23% depending on the f_y value. In the 2006 version of the Concrete Standard (NZS 3101), Eq. 5 was introduced as a specific limit for minimum vertical reinforcement in walls. For a 30 MPa concrete strength, Eq. 5 results in ρ_l between 0.27 and 0.46% depending on the reinforcing steel grade. It should be noted that Eq. 5 was adapted from the equation previously derived for minimum longitudinal reinforcement in beams, with the area of tension reinforcement in beams substituted for the area of total vertical reinforcement in walls. For beams, the equation was intended to ensure that there was a margin of safety between the likely cracking moment and the section flexural strength.

$$\rho_l \geq \frac{\sqrt{f_c'}}{4f_y} \tag{5}$$

where f_c' is the specified concrete compressive strength in MPa, and f_y is the yield strength of the reinforcing steel in MPa.

The results of moment-curvature analysis conducted by Henry (2013) have highlighted several deficiencies of Eq. 5. This equation was developed for beams with top and bottom layers of reinforcement only and fails to account for the distributed reinforcement in walls, slenderness of wall sections, size effects, aspect ratio and axial loads. Walls designed with minimum vertical reinforcement in accordance with Eq. 5 may be vulnerable to sudden failure unless a significant axial load exists. As shown subsequently, inelastic deformations in these walls will be concentrated at a limited number of cracks as opposed to distributed cracking, resulting in smaller effective plastic hinge lengths that are typically assumed for ductile concrete walls.

FIELD OBSERVATIONS

As indicated, advancements to design provisions have been continuously made in seismic regions throughout the world, especially since the 1970s. Field observations, large-scale testing, and improved analysis capabilities have generally contributed to these advancements. In this context, such advancements and their implementation in practice have been more rapidly accomplished in New Zealand, particularly for concrete structures. This was possible partly due to a relatively small but effective earthquake engineering community and the close interaction between the academic researchers and practicing engineers. Consequently, the Central Business District (CBD) of Christchurch served as a good test bed to verify the performance of improved design methods and detailing adopted for concrete walls.

Prior to presenting the damage to concrete walls, a brief discussion on the assumed seismicity of Christchurch and recorded ground motions in the 2010/2011 Canterbury earthquakes is warranted. Prior to the 2010/2011 earthquakes, seismic hazard in Christchurch was considered to be moderate; the peak ground acceleration (PGA) of the 500-year elastic design spectrum corresponding to deep soil sites was 0.22g. The first of the Canterbury event, the Darfield earthquake, occurred on September 4, 2010, with a moment magnitude, M_w, of 7.1. With an epicenter approximately 35 km west of Christchurch, this event caused damage primarily to unreinforced masonry buildings in the CBD. A typical sequence of aftershocks followed this event although it was later found that some of these events occurred in smaller faults closer to the city (Hare et al. 2012). The most damaging event of this

sequence was the 2011, M_w 6.3, Christchurch earthquake that occurred on February 22nd, 2011, at a depth of 5 km and a distance of about 10 km from CBD. A series of aftershocks ensued this event including 20 of them with M_w of 5 or greater. The duration of strong shaking for the September event was estimated to be 15 seconds and the corresponding value for February event was about 7 seconds. The spectra from the September event were noted to be comparable to the design spectra, while the February event produced considerably higher spectral accelerations than those expected for a design level earthquake.

The maximum recorded peak accelerations in the Christchurch earthquake were 2.2g and 1.7g in the vertical and horizontal directions, respectively, with horizontal PGAs exceeding 0.7g around the CBD based on four recorded motions within 1.5 km of CBD (McVerry et al. 2012). The elastic spectra corresponding to the recorded ground motions from these sites were about twice the 500-year return period design spectrum and were stronger than the spectra for return periods of 2500 years. Therefore, the buildings in CBD were subjected to high intensity, short-duration horizontal ground motions during the Christchurch earthquake. What is also apparent is that the vertical motion was strong even during the strong horizontal shaking due to the close proximity of the CBD to the earthquake source.

A general field observation is that a variety of buildings with concrete walls achieved their life-safety design objectives in the Christchurch earthquake. Although many buildings showed only minor damage, severe damage and undesirable failures were identified for a number of concrete walls. Given the short duration and relatively small number of excursions with large accelerations, the observed wall damage is likely to have occurred rapidly. Minimal damage limited to formation of a few flexural cracks and no spalling of cover concrete in the plastic hinge region support the hypothesis that failure of concrete walls occurred in a brittle manner although they had been designed to develop ductile response. If the walls had performed as expected, the wall base would have accommodated the required inelastic demand and numerous flexure and flexure-shear cracks over a height of about 0.5 to 1.0 times the wall length.

An overview of wall damage in the Christchurch earthquake may be realized from **Figure 4,** which shows the result of rapid building safety evaluations that was conducted during the national state of emergency immediately following the Christchurch earthquake (Kam et al. 2011). This figure shows three categories of damage distribution as a function of design era. Accordingly, red indicated unsafe to enter, yellow corresponded to restricted entry and green

indicated unrestricted entry though a detailed evaluation was still needed. An underlying assumption here is that access to building reflects the extent of damage to concrete walls. In this context what is important to realize is that the modern wall buildings, designed after the 1990s, show approximately two times the red category as the pre-1980 buildings and three times as many as the 1980s. It is also worth noting that as of the writing of this paper about 60% of the multi-story buildings with reinforced concrete walls in the CBD have been demolished, which is likely to have included most of the red and yellow placarded buildings.

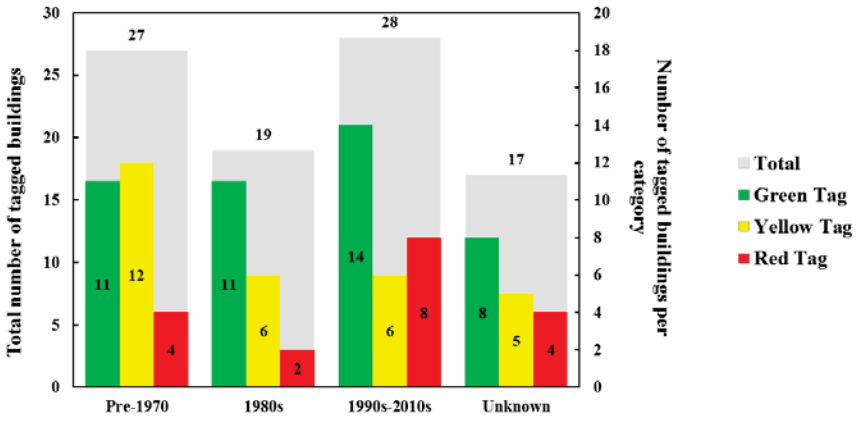

Figure 4 An overview of damage to concrete walls building based on rapid safety evaluation data (after Kam et al. 2011)

Anecdotally, the 1980s walls were designed with two layers each for the vertical and horizontal reinforcement and their typical thickness ranged from 300 to 500 mm. They were often designed with boundary elements with large vertical and confining reinforcement ratios to increase the robustness of the walls for resisting earthquakes. From 1990 onwards, an increasing number of relatively thin (less than 200 mm thick) load bearing walls with one layer of both vertical and horizontal reinforcement have been built without boundary elements. A number of such modern walls performed poorly in the earthquake. Pre-1980, the necessary detailing of the 1980s (in the boundary elements) was not employed and probably accounts for the increasing need for red placards. Typically, these walls used 200-250 mm or greater wall thickness.

WALLS WITH LIMITED DAMAGE

The concrete wall shown in **Figure 5** experienced noticeable distress due to the earthquake motion. Three observations from this figure are: (a) The intensity of ground motion at this site was significant enough to cause cracking but not spalling of cover concrete in the plastic hinge region near the wall base; (b) Use of increased longitudinal reinforcement

in the end regions of wall seems to have controlled the crack width in these regions; and (c) Relatively wider cracks with large spacing apparent on the wall surface in the web regions confirm the use and possible consequence of lightly reinforced concrete in that region. **Figure 6** shows a concrete wall in a 14 story hotel building that had well distributed flexural cracking. As described by Wilson and Lewis (2011), the plastic hinge region in this case was located above level 4 where the building footprint was reduced. The 8 m long and 0.3 m thick wall was designed in accordance with current NZS 3101 standards (2006) and had 1 m long boundary elements with a ρ_l of 2.7% and the web region contained well-distributed longitudinal reinforcement with a ρ_l of 1.0%. The resulting crack widths were between 0.5-0.8 mm and the wall was easily repaired.

Figure 5 Observed distress to a concrete wall with minimal damage (Photos: Courtesy of Elwood)

Figure 6 Well-distributed flexural cracks on a wall (Wilson and Lewis 2011)

WALLS WITH HIDDEN DAMAGE

In ductile concrete walls, a plastic hinge is expected to form at the wall base when subjected to seismic loading. While this is typical of what has been seen in many tests in laboratories around the world (e.g., **Figure 1** and **Figure 2**), formation of significantly fewer

cracks in the plastic hinge zones occurred in many walls in Christchurch. Based on the proximity of buildings to the epicenter, the plastic strains in some walls were expected to be large. However, fracture of several longitudinal bars in the wall end regions—as observed in the field—was unexpected. This observation is attributed to the formation of fewer cracks in the plastic hinge than those expected from during typical laboratory tests.

Two examples of this type of wall behavior were observed in multi-story Gallery Apartment building built in 2006 (see **Figure 7** and **Figure 8**). Damage to both walls was characterized by formation of only few flexural cracks in the plastic zone. In the first example (see **Figure 7**b), it appears that the cover concrete spalled off first followed by the buckling of the longitudinal reinforcement. **Figure 8** shows the second example, in which a wall with a single flexural crack and fracture of multiple longitudinal bars is seen. This type of damage was particularly concerning due to the fact that the fractured bars were hidden behind what appeared to be relatively minor damage. Subsequent reports prepared by CERC (2012) and Smith and England (2012) highlighted several deficiencies in the Gallery Apartment building including a mismatch in the assumed ductility and wall detailing. Additionally, the walls in the building were designed prior to the introduction of more stringent minimum vertical reinforcement limits in NZS 3101 (2006). The grid-F wall shown in **Figure 8** had a total vertical reinforcement ratio of 0.16%; only 55% of the vertical reinforcement required by NZS 3101 (2006). The low vertical reinforcement content combined with measured concrete strengths that were significantly higher than the specified strength likely contributed to the observed lack of flexural cracking.

(a) Overall view (b) Wall damage

Figure 7 Observed distress to a concrete wall in a multi-story apartment building (Courtesy of Elwood)

(a) Concrete removal (b) Fractured bar

Figure 8 Unexpected damage to another wall in the building shown in Fig. 7a

WALLS WITH SIGNIFICANT DAMAGE

A number of walls, including those that appeared to have good reinforcement details, suffered buckling in the plastic zone. As previously discussed, the cyclic combination of large tension strains and subsequent compression can trigger local wall buckling. This issue is exacerbated when walls are designed with boundary elements and lightly reinforced web regions. **Figure 9** shows a 7-story reinforced concrete wall structure built in 1984, which comprised of two L-shaped walls. The wall on the north experienced significant damage to concrete just adjacent to a boundary element and out-of-plane buckling of the boundary element. The longitudinal steel ratios in the boundary element and outside of the boundary element were estimated to be about 2% and 0.12%, respectively. While 0.12% is lower than the current minimum vertical reinforcement ratio, this amount is consistent with the minimum requirement of the era when the building was designed.

(a) Overall view (b) Damaged north L wall

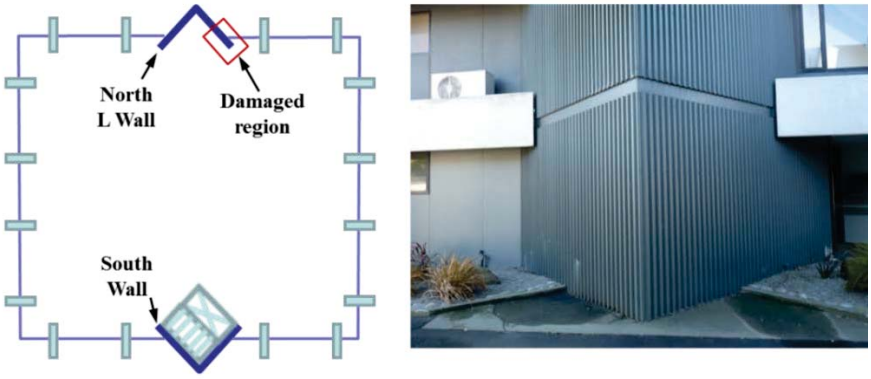

(c) Plan view (after Elwood 2011) (d) Undamaged south L wall

Figure 9 A seven-story office building with wall damage

The lack of damage to the south L wall may be attributed to the building not being as well connected to that wall due to stair and lift shaft penetrating through the diaphragms, adjacent to the wall. In **Figure 9**d, the back of the south L wall is shown, which shows virtually no damage to this wall. A similar observation was made on the inside faces of this wall.

Likewise, the interior of the building also showed limited damage, including to the non-structural elements.

As seen in **Figure 10**, failure of lapped splices in reinforcing bars caused signifcant wall damage in a 13 story apartment built in 1999. This building also used a combination of a long coupled (L = 10 m) and short (L = 3 m) walls in the building configuration, with signifciant damage ocurring only to the long wall. The vertical reinforcement was spliced over part of the wall length with the damage concentrated about the splice. The severly damaged region also had poorly detailed horizontal (or shear) reinforcement and a lack of ties between the two layers of reinforcement in the web region. As shown in **Figure 10**c, the horizontal reinforcement was terminated with a 90 degree bend that was not anchored into the confined boundary element, and the shear reinforcement was also lapped in the cover concrete, which pulled out when the wall was damaged. Since the lap splice was not in the plastic hinge region, this issue is not further investigated. However, specific failure of walls as in **Figure 10** would be worthwhile studying in detail in the future.

(a) The building complex (b) 10 m wall - failure above the spliced region (c) Poor anchorage of horizontal reinforcement (d) Lapped shear reinforcement

Figure 10 Performance of a concrete wall in one building of the Terrace on the Park

ANALYSIS OF WALLS

Considering the field observations of the performance of concrete walls in Christchurch and concerns raised previously with regards to the current design practice, this section is devoted to analysis of concrete walls to provide rationale for advancing seismic design of walls and to help formulate design recommendations.

DISTRIBUTION OF LONGITUDINAL REINFORCEMENT

To further understand the impact of longitudinal reinforcement layout on the wall performance, a series of detailed finite elements analyses was undertaken. For this purpose, VecTor2, developed at the University of Toronto, was used due to its ability to capture flexural and shear deformations (Wong and Vecchio, 2002). Previous studies on the distribution of longitudinal reinforcement in walls (e.g., Priestley and Kowalsky, 1998; Dai,

2012) were based on section analyses and therefore the axial strain in concrete and longitudinal reinforcement was due to flexure and axial load only. Using a 2.0-m long, cantilever wall test unit WSH3 that was subjected to quasi-static cyclic loading by Dazio et al. (2009), the analysis capability of VecTor2 was first verified. The wall was loaded using a horizontal actuator positioned 4.56 m above the wall base, applying cycles of horizontal displacements with increasing amplitude. The reinforcement layouts of the wall are shown in **Figure 11**a. The test unit was subjected to a constant axial force of 686 kN (or an axial load ratio of 0.058). The wall was capacity-designed and failed due to crushing of the well-confined boundary element after reaching displacement ductility of 6. In the numerical model, longitudinal and shear reinforcement was modeled as smeared reinforcement considering the Bauschinger effect in the hysteretic response. The concrete compression was modeled assuming a parabolic stress-strain relationship (Wong and Vecchio, 2002), but the concrete tension stiffening was not included.

Figure 11b compares the numerical force-displacement response to that obtained during testing, which confirms that the numerical model captures both the overall force-displacement response and the cyclic hysteretic behavior with good accuracy. **Figure 11**c compares the ratio of shear to flexural deformation components, which shows appropriate representation of flexure and shear components in the numerical model when compared to the experimentally determined shear to flexural deformation ratios using two different methods (i.e., Hiraishi's method (1984) and indirect method in Beyer et al., 2011), which also confirms satisfactory behavior of the analytical model.

Next, two further wall analyses were conducted. Both used the same dimensions as WSH3, with longitudinal reinforcement concentrated in the boundary elements in the first case (identified as WSH3-C) and distributed along the wall length in the second case (identified as WSH3-D). **Figure 12** shows the two reinforcement layouts, which were chosen to produce comparable flexural resistance with an axial load of 686 kN. As a result, the total ρ_l of the wall with distributed reinforcement was about 15% higher than that of the wall with concentrated reinforcement. The reinforcement ratios of the boundary elements and the web of the two walls are summarized in **Table 1**. Using capacity design principles, identical shear reinforcement and stirrup layout were adopted for both walls.

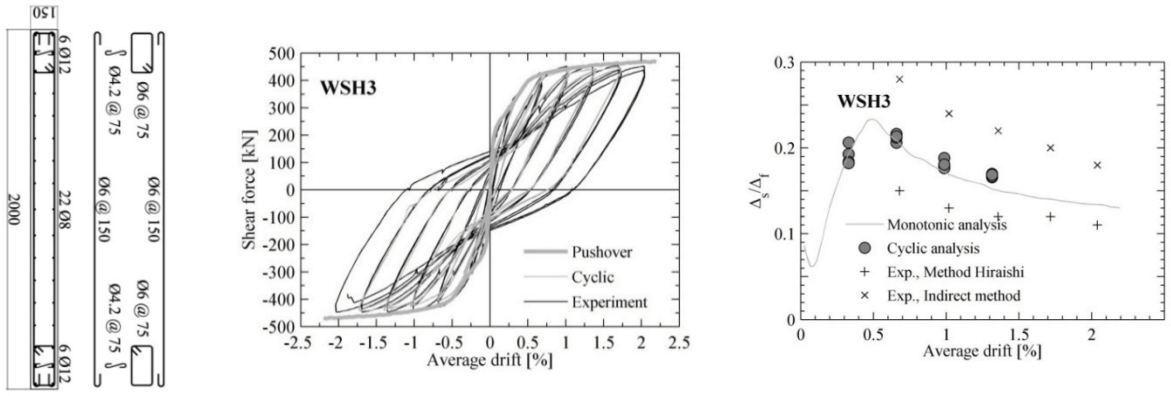

(a) (b) (c)

Figure 11 Wall WSH3 tested by Dazio et al. (2009) and comparison of its simulated response using a VecTor 2 model to experimental data: (a) Reinforcement layout (b) Force-displacement response (c) Ratio of shear to flexural deformations

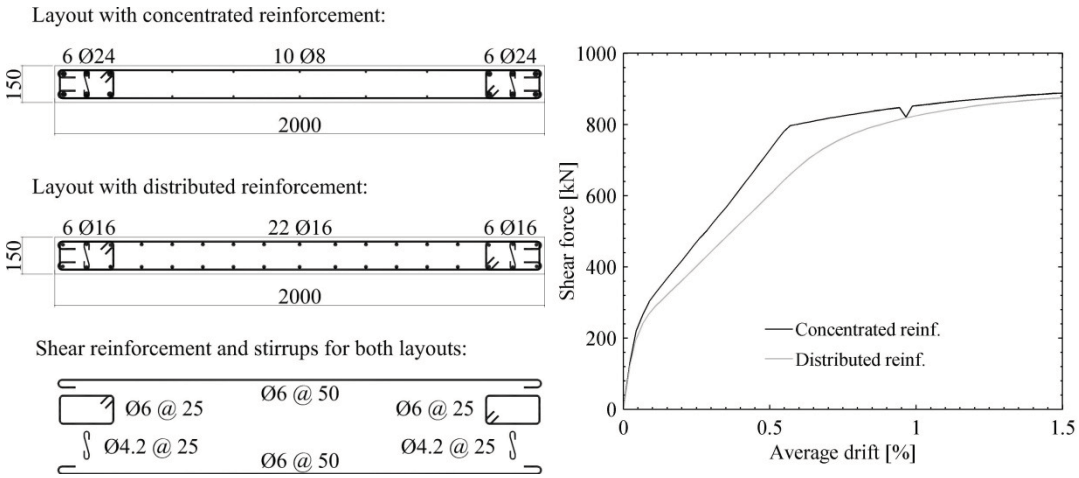

(a) Cross sections and reinforcement layouts (b) Monotonic force-displacement responses

Figure 12 Comparison of two hypothetical walls: WSH3-C vs. WSH3-D

As targeted, both walls provided a similar shear and base moment resistance (see **Figure 12**b, **Table 1**). **Figure 13** shows the force-displacement responses obtained for the two hypothetical walls subjected to both monotonic and cyclic loading. While both cyclic analyses appear to produce stable hysteretic responses up to 1.3% drift, WSH3-C failed at this point due to sliding failure at the large base crack. This failure mode was preceded by short branches of almost zero lateral stiffness during unloading and reloading response of WSH3-C in the previous load cycles. When compared to WSH3-D, WSH3-C resulted in somewhat broader hysteresis loops, indicating development of larger inelastic steel strains and therefore a small increase in energy absorption capacity at a given drift. This difference in energy absorption will have, however, only relatively small impact on the peak displacement demand during an earthquake (Priestley, 2003).

Table 1 Comparsion of longitudinal reinforcement ratios in the three walls and nominal shear resistance according to ACI 318 and NZS 3101

Wall ID	ρ_l in boundary element	ρ_l in web	Average ρ_l in wall	ρ_v	$V_{n,shear}$ [1)] ACI 318^{2011}	$V_{n,shear}$ [1)] NZS 3101^{2006}
WSH3	1.74%	0.50%	0.82%	0.25%	703 kN	590 kN
WSH3-C	6.96%	0.23%	1.98%	0.75%	1250 kN	1690 kN
WSH3-D	2.28%	2.28%	2.28%	0.75%	1250 kN	1690 kN

[1)] Computed with mean values of f_y and f_c'

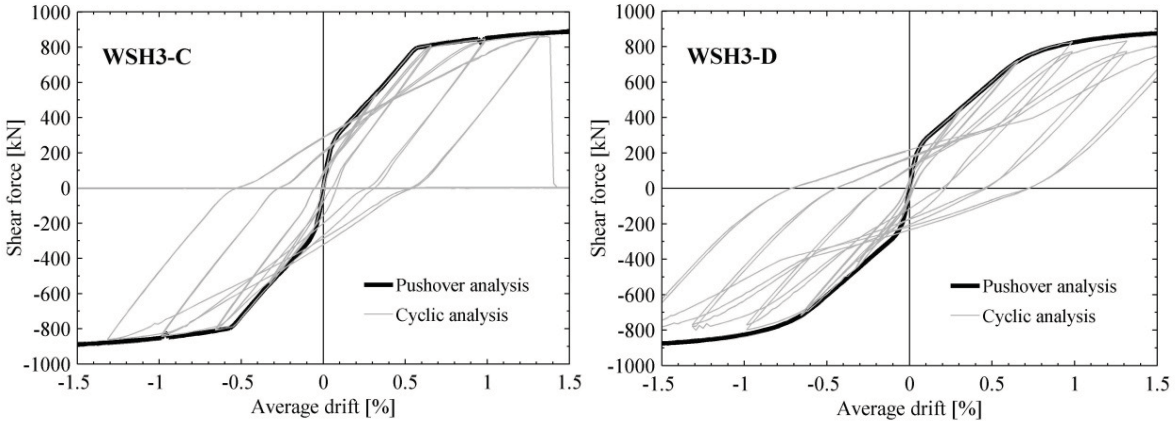

(a) WSH3-C (b) WSH3-D

Figure 13 Comparison of simulated force-displacement responses

Similar to the damage pattern shown in **Figure 1**, formation of wide cracks in the lightly reinforced web region is observed for WSH3-C at the base in **Figure 14**a. In the boundary elements with a large ρ_l, the crack widths are much smaller. For the same top lateral displacement, the maximum crack width in WSH3-D is about one third of the maximum crack width observed in the web of WSH3-C (**Figure 14**b). As a result, the wall will be less prone to sliding shear failure, rupture of the longitudinal reinforcement bars, web crushing and separation of boundary elements from the web. A concentration of damage to the web for walls with heavily longitudinal reinforcement in the boundary elements and lightly reinforced webs was also observed in the field (e.g., **Figure 9**) and in experimental research (**Figures 1** and **2**a).

Distributing the longitudinal reinforcement along the length of the wall also facilitated a better control of the shear deformations in the plastic zone of the wall. **Figure 15**a shows the ratio of the shear to flexural deformations for the monotonic analyses. Accordingly, the ratio of shear to flexural wall deformations of WSH3-C is about 20% larger than those obtained

for WSH3-D. Due to the large crack widths, the shear stiffness of WSH3-C is noticeably reduced although the wall had adequate shear reinforcement, leading to larger shear strains in the plastic zone of WSH3-C than WSH3-D. This is illustrated in **Figure 15**b by using shear deformations and shear strains obtained at zero top lateral displacement after the end of the second cycle to 1.0% drift.

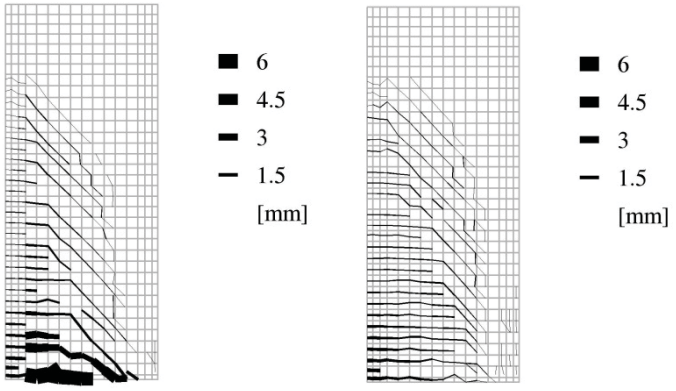

(a) WSH3-C (b) WSH3-D

Figure 14 Observed crack pattern at 1% lateral drift

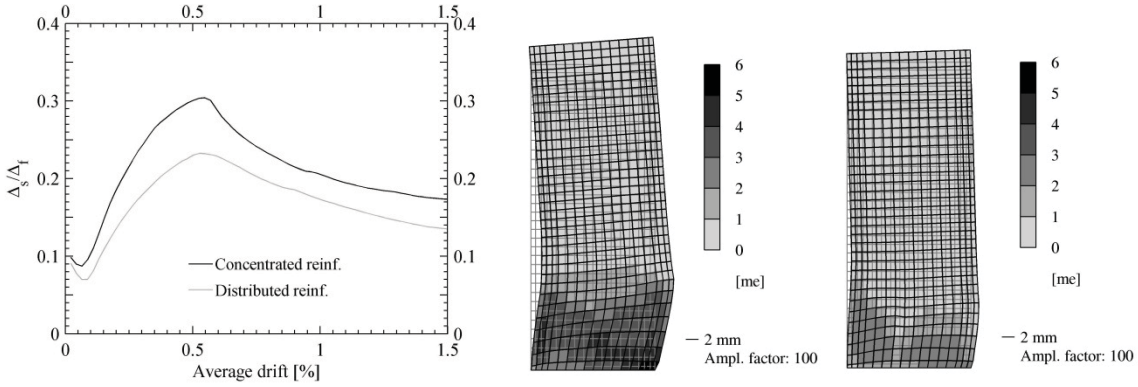

WSH3-C WSH3-D

(a) Ratio of shear to flexural deformations (b) Deformed shapes and shear strains

Figure 15 Comparison of shear deformations obtained for WSH3-C and WSH3-D

WALL BUCKLING

To understand the out-of-plane buckling potential of walls and associated instability resulting from large tension demand on the longitudinal reinforcement, a parametric study was undertaken to identify the importance of key design variables identified earlier (see Eqs.

1 – 4). In this effort, wall thickness, length, height, longitudinal and transverse steel ratios, plastic hinge length, L_P, as a % of that given by Eq. 6, and concrete strength were used as variables as summarized in **Table 2**.

$$L_P = k \cdot H_e + 0.1L + L_{SP} \tag{6}$$

where $k = 0.2(f_u/f_y - 1) \leq 0.08$; $L_{SP} = 0.022\, f_y\, d_b$; f_y and f_u are, respectively, yield and ultimate strength of longitudinal reinforcement in MPa; and H_e is the wall effective height and taken as 2/3 of total wall height. Also, l_o in Eqs. 1 and 4 were equated to L_P.

Table 2 Variables considered in the wall bucking parameter study

Variable			Typical				
Wall thickness, b (m)	0.1	0.2	0.3	0.4			
Wall length, L (m)		2	3	6	8		
Wall Height, H (m)		5	10	15	20		
Concrete strength		30	35	40			
Longitudinal steel ratio (%)		0.5	1.0	1.5	2.0	2.5	3.0
Transverse steel ratio (%)		0.5	1.0	1.5			
L_P (% of Eq. 6)	50	75	100	125	150		

In terms of importance, it was found that wall geometric properties (i.e., b, L and H) had the greatest impact on results. Possible variability of L_P also had a significant impact. Consider **Figure 16**, which represents the results of the study with regards to impact of wall height, length and thickness. **Figure 16**a and b depict the relationship between cantilever wall top displacement and steel tension strain as obtained from a moment-curvature analysis for walls of height 5, 10, 15, and 20 m and wall thicknesses of 100, 200, 300, and 400 mm. Note that the lines in each figure represent the average responses obtained for the two different wall thicknesses since they were relatively close to each other. Superimposed on these graphs are the limit strains predicted by both the Paulay and Priestley (1993) and the Chai and Elayer (1999) stability models. Also shown in the graphs are approximate values for serviceability (defined using a concrete compression strain of 0.004 or a steel tension strain of 0.015, whichever occurred first), damage control (defined using Eq. 7 as suggested by Paulay and Priestley (1992) or a steel tension strain of 0.06, whichever occurred first), and ultimate limit states (defined using a concrete compression strain of 1.5 times Eq. 7 or steel tension strain of 0.09, whichever occurred first).

$$\varepsilon_{cu} = 0.004 + 1.4\rho_s f_{yh} \varepsilon_{sm} / f_{cc}^{'} \quad (7)$$

where ρ_s is volumetric ratio of the confining steel, ε_{sm} is the steel strain at the maximum tensile stress, f_{yh} is the yield strength of confining steel, and $f_{cc}^{'}$ is the confined concrete strength as suggested by Mander et al. (1988). Each moment curvature analysis was carried out for strains much greater than what would actually be sustained. This was done since in some cases the stability strains predicted by the models were significantly greater than the concrete and steel strains corresponding to the ultimate limit state.

From **Figure 16**, the importance of wall thickness and height on the stability strain is evident, and follows the expected trend, i.e., thinner and taller walls are more likely to suffer out of plane stability due to in-plane forces. According to the stability models discussed in this paper, if that failure mode is to be avoided, walls thickness of at least 400 mm would be required for 20 m tall walls, and 200 mm thick walls would be required for 5 m tall walls. In all cases, this data was for a wall of 4 m in length. **Figure 16**c and d represent similar data for 10-m tall walls as a function of wall length, which show that walls of longer length are more likely to suffer from out of plane stability due to in plane loading. The data shown in **Figure 16** assumes an axial load ratio of $0.1f_c'A_g$ in the displacement calculation. Note that the critical tensile strain for both buckling models, i.e., Eqs. 1 and 4, are independent of the wall axial load ratio. But the calculation of wall lateral displacements at a given level of strain is impacted by the axial load ratio since changes in the axial load will impact the neutral axis depth, which in turn affects the curvature and hence the displacement. Thus any axial load ratio different from the assumed $0.1f_c'A_g$ is expected to influence the strain-displacement relationships and the displacements at the onset of buckling presented in **Figure 16**. Different values of axial load ratio would simply result in a different scale applied to the vertical axis.

The results of these analyses should be considered within the context of current code limits on wall aspect ratio that are used to control global wall buckling. To assure that local wall instability resulting from large tensile strain in the longitudinal reinforcement is avoided, it is important to develop limits on aspect ratio as a function of key design variables such as ϵ_{sm}, b, L, H, L_P, and ρ_l.

MINIMUM LONGITUDINAL REINFORCEMENT

Detailed finite element analysis was also completed to investigate the failure of one of the RC walls in the Gallery Apartment building in Christchurch. As shown in **Figure 8**, the RC

wall on the east face of the building experienced a single concentrated crack at the wall base with fractured vertical reinforcement. This wall, which was described as the grid-F wall in the report prepared for the Canterbury Earthquakes Royal Commission by Smith and England (2012), was 4300 mm long, 325 mm thick, with a total height of 39 m. The vertical and horizontal reinforcement consisted of two layers of 12 mm diameter grade-500 bars at 460 mm and 400 mm centers, respectively. The axial load from the self-weight of the wall and the tributary floor area was equal to 2250 kN.

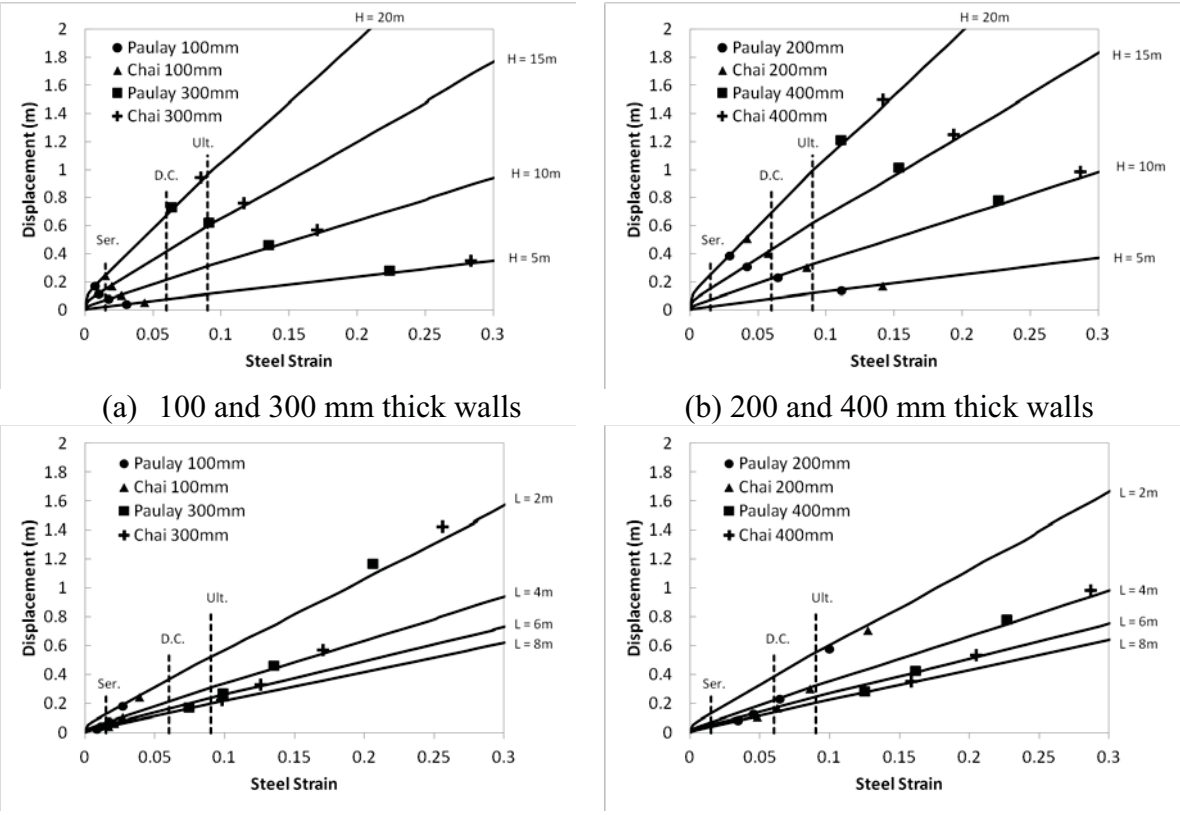

(a) 100 and 300 mm thick walls

(b) 200 and 400 mm thick walls

(c) 100 and 300 mm thick walls

(d) 200 and 400 mm thick walls

Figure 16 Stability analysis of walls of varying thicknesses, heights and lengths

The as-built grid-F wall was also modeled using VecTor 2, with the vertical and horizontal reinforcement as smeared reinforcement and the following average measured properties: yield strength of 560 MPa, ultimate strength of 690 MPa, and ultimate strain of 12.9%. A concrete compressive strength of 51.3 MPa was used based on the average strength measured from cores extracted from the building. The corresponding tensile strength was calculated as 4.34 MPa based on the fib recommendations (fib model code, 2010). The wall was subjected to a monotonic lateral displacement at a height of 26.1 m, equivalent to the center of an inverse triangular lateral load distribution.

The crack pattern and lateral force-displacement response from the finite element analyses of the as-built grid-F wall are shown in **Figure 17**. The analytical crack pattern correlated well with the observed performance of the wall, with cracking concentrated at a single primary crack at the wall base with no secondary crack formation. The wall response was elastic until the first crack developed at a lateral force of 205 kN and the peak strength was reached at a lateral drift of 0.7% before fracture of the vertical reinforcement occurred. The analysis confirms the findings of other reports that concluded based on section analyses that the vertical reinforcement content in the grid-F wall of the Gallery Apartments building was insufficient to initiate secondary cracking, resulting in a concentration of inelastic actions at the wall base (CERC 2012; Henry 2013).

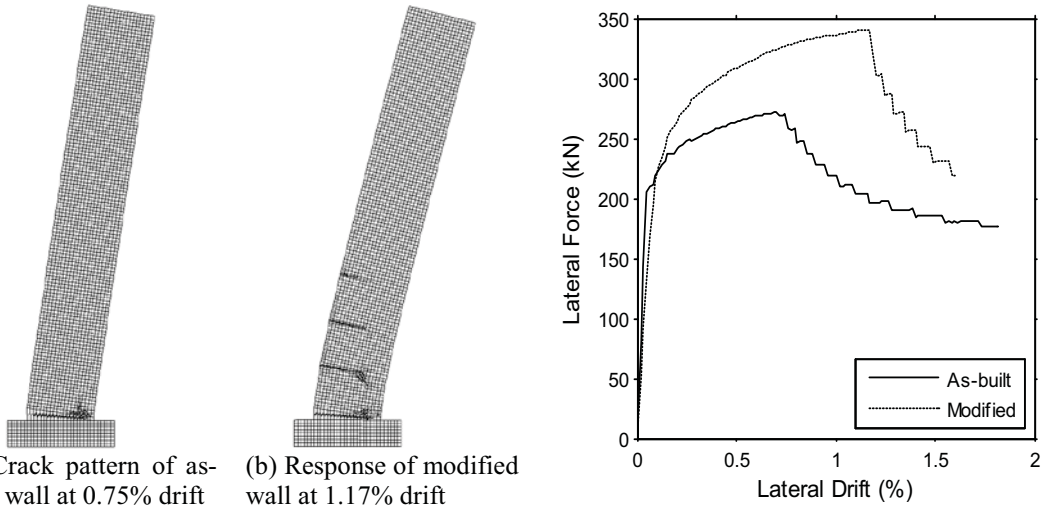

(a) Crack pattern of as-built wall at 0.75% drift

(b) Response of modified wall at 1.17% drift

(c) Lateral force-displacement

Figure 17 Predcited response of grid-FEM wall

A further analysis of the grid-F wall was conducted with an increased vertical reinforcement to comply with the current limits in NZS 3101:2006 (i.e., Eq. 5). Using the specified concrete strength of 30 MPa, the resulting vertical reinforcement content of 0.274% was used. Additionally, the 30 MPa specified concrete strength with a corresponding tensile strength of 2.9 MPa was used. The resulting crack pattern and lateral force-displacement results of the modified grid-F wall are also shown in **Figure 17**. Instead of a single crack at the wall base, four primary flexural cracks were obtained for the modified grid-F wall with minimal secondary cracking. Both the lateral strength and drift capacity increased with the additional reinforcement before fracture of the vertical reinforcement occurred. These results confirm that although the wall performance would have been improved if current levels of

minimum vertical reinforcement were used, a lack of well distributed secondary cracks and premature fracture of the vertical reinforcement would still be expected.

DESIGN RECOMMENDATIONS EMERGING FROM OBSERVED DAMAGE

Following the earthquake damage in Christchurch, there has been significant effort placed on improving design standards. This section examines the relevant recommendations published by the Structural Engineering Society of New Zealand (SESOC 2012) and the Canterbury Earthquakes Royal Commission (CERC 2012) and offers further suggestions.

DISTRIBUTION OF VERTICAL REINFORCEMENT

With regards to improving ductile wall performance, one specific recommendation by CERC and SESOC was that confinement in the boundary region should be provided over the full length of the compression region. With respect to the web regions of the reinforcement, it is recommended that transverse reinforcement in the central portion of the wall should satisfy the anti-buckling requirements. Except for walls with minimum longitudinal reinforcement (see details below), no recommendation regarding the distribution of the longitudinal reinforcement in the wall section was made. Based on the cited previous work and the test observations, it is suggested that 40% of the total longitudinal reinforcement be placed within the web as opposed to placing heavy vertical reinforcement in the end regions. Maintaining the amount of ρ_l in the boundary elements while strengthening the web region is also acceptable, but this approach will increase the lateral load capacity of the wall unnecessarily, thereby increasing foundation loads and other design forces in accordance with capacity design principles.

WALL AND BAR BUCKLING

In response to observed buckling of plastic hinge regions in several concrete walls and buckling of vertical reinforcement, SESOC and the CERC have suggested stricter detailing. In addition to the confinement requirement and anti-buckling requirements noted above, it is suggested that for walls with an axial load ratio greater than 0.1, the ratio of clear height to wall thickness should not exceed the smaller of 10, or the value derived from NZS 3101:2006 clause 11.4.2, which is based on the Paulay and Priestley equation but without a dependency on an expected maximum tensile strain. Furthermore, recommendations for stricter wall slenderness limits have also been suggested by several other researchers. Based on observations from the 2010 Chilean earthquake, Wallace et al. (2012) suggested that the

adoption of a story height to wall thickness limit should be considered, such as the limit of 16 in the 1997 Uniform Building Code UBC). Moehle et al. (2011) recommended a slenderness limit of 10 within the intended plastic hinge region and 16 as per UBC elsewhere.

Based on the wall bucking analysis and discussion presented herein, it is strongly recommended that minimum wall thickness required to prevent instability be linked to estimated tensile strains in the longitudinal reinforcement at the wall base. This requirement should be added in addition to any requirements that are used to prevent global wall buckling resulting from axial compression of slender walls. Furthermore, the minimum wall thickness requirement should not be limited to walls subjected to large axial load ratios. In lightly loaded walls, wider crack widths and larger tensile strains should be expected, making them more vulnerable to out-of-plane instability under reversed loading.

MINIMUM VERTICAL REINFORCEMENT

To improve ductile performance of walls with minimum vertical reinforcement which are designed with uniformly distributed longitudinal reinforcement, SESOC and CERC have recommended increasing the current minimum vertical reinforcement by a factor of 1.6 to account for the actual concrete compression strength being up to 2.5 times greater than the specified concrete strength. CERC also recommends changes to the distribution of the reinforcement in the wall. In this regard, SESOC has noted that vertical reinforcement should be lumped at the ends of the wall with minimum reinforcing distributed along the web region. This suggestion contradicts the findings regarding the reinforcement distribution presented earlier in this paper. However, that investigation focused on walls with large longitudinal reinforcement ratios. A further investigation should be undertaken before deciding the best reinforcement distribution method for walls with minimum reinforcement ratios.

As highlighted by the analysis presented in this paper, the observations of buildings such as the Gallery Apartment building should be interpreted with caution as the vulnerability was exacerbated by vertical reinforcing contents being significantly less than that required by current design standards. Nonetheless, CERC, Henry (2013), and the analysis presented in this paper have illustrated that even when the concrete strength is known, the current minimum vertical reinforcement limits in NZS 3101 (i.e., Eq. 5) may not be adequate to ensure well distributed cracks form in the plastic hinge region. This concern stems from the use of Eq. 5 and the inability of commonly used section analysis methods to include the effects of crack distribution.

There are also other concerns that need to be systematically investigated. For example, by studying deep beams, Carpinteri and Corrado (2011) have suggested that minimum flexural cracking strength of concrete is influenced by member depth, suggesting the dependency of Eq. 5 on wall length. This issue has been identified in the fib model code and commentary section of NZS 3101 (2006), but without any implication to design practice. As recommended by CERC, further investigations in this area are needed to develop more robust provisions for minimum reinforcement requirements.

CONCLUSIONS

Following a noticeably large number of failures of concrete walls that were designed to behave in a ductile manner in the Christchurch earthquake, this paper was dedicated to investigating potential causes of less obvious wall failures and identifying means to improve their performance. In this process, findings from past research and additional analyses were used to investigate four specific issues and the following conclusions were drawn:

- Whether it is required by design codes or not, concrete walls in seismic regions are often designed with boundary elements containing heavy longitudinal reinforcement ratios and lightly reinforced middle regions. Even if these walls are not susceptible to out-of-plane stability problems, the use of minimal reinforcement in the web will lead to undesirable consequences. It is recommended that distributing the reinforcement along the wall length with proper confinement in the compression zone will improve seismic performance of walls at large displacements and minimize shear deformations. Although experimental validation is required, it is suggested that at least 40% of the total longitudinal reinforcement be used in the web.

- Wall out-of-plane instability resulting from large tensile strains developing in the longitudinal reinforcement at the wall base can be controlled by appropriately choosing the wall thickness. Only the NZS 3101 (2006) uses this concept in deciding the wall thickness, but its simplified approach makes the minimum wall thickness independent of the maximum expected longitudinal tensile steel strain. It is concluded that wall design should include a minimum wall thickness calculation directly based on Eq. 1.

- Walls designed with current-code based minimum vertical reinforcement may not behave in a ductile manner. Further research is required to confirm the seismic behavior of lightly reinforced concrete walls and provide guidance on the required minimum

vertical reinforcement. An appropriate amount needs to be established taking into account realistic concrete strengths, dependency of tensile strength on wall length and other influencing parameters.

ACKNOWLEDGEMENTS

The first author of this paper is grateful to the financial support and opportunity provided by the Earthquake Engineering Research Institute for participating in the reconnaissance work of the 2011 Christchurch earthquake. MS Student Kelly Herrick of North Carolina State University was responsible for the data and figures relating to the wall stability parameter studies and PhD student Yiqiu Lu of the University of Auckland was responsible for the data related to the analysis of the Gallery Apartment grid-F wall. The authors also greatly appreciate the detailed and valuable feedback provided by three anonymous reviewers and an associate editor, which certainly improved the quality of the paper.

REFERENCES

Aaleti, S., Brueggen, B.L., Johnson, B., French, C., Sritharan, S., 2013. Cyclic response of RC walls with different anchorage details: An experimental investigation. *ASCE Journal of Structural Engineering* **139** (7): 1181-1191.

ACI Committee 318, 2011. Building Code Requirements for Structural Concrete (ACI 318-11). American Concrete Institute, Farmington Hills, MI.

Beyer, K., Dazio, A. and Priestley, M. J. N., 2008. Quasi-static cyclic tests of two U-shaped reinforced concrete walls, *Journal of Earthquake Engineering* **12** (7), 1023-1053.

Beyer, K., Dazio, A. and Priestley, M. J. N., 2011. Shear deformations of slender reinforced concrete walls under seismic loading, *ACI Structural Journal* **108** (2), 167-177.

Brueggen, B. L., 2009. *Performance of T-Shaped Reinforced Concrete Structural Walls Under Multi-Directional Loading*, Ph.D. Thesis, University of Minnesota, Twin Cities, MN, 499 pp.

Canterbury Earthquakes Royal Commission (CERC), 2012. Final report: Volume 2: The performance of Christchurch CBD buildings. http://canterbury.royalcommission.govt.nz/Commission-Reports, Wellington, New Zealand.

Carpinteri, A., and Corrado, M., 2011. Upper and lower bounds for structural design of RC members with ductile response, *Engineering Structures*, **33** (12), 3432–3441.

CEN, 2004 *Eurocode 8: Design of structures for earthquake resistance – Part 1 General rules, seismic actions and rules for buildings*, European Committee for Standardization, Brussels, Belgium.

Chai Y. H. and Elayer, T. D., 1999. Lateral stability of reinforced concrete columns under axial reversed cyclic tension and compression, *ACI Structural Journal* **96** (5), 780-789.

Dai, H., 2012. *An Investigation of Ductile Design of Slender Concrete Structural Walls*, MS Thesis, Iowa State University, Ames. IA, 134 pp.

Dazio, A., Beyer, K., and Bachmann, H., 2009. Quasi-static cyclic tests and plastic hinge analysis of RC structural walls, *Engineering Structures* **31**, 1556-1571.

Fédération Internationale du Béton (fib), 2012. Model Code 2010 - Final draft, Volume 1. fib Bulletin No. 65, Lausanne, Switzerland.

Goodsir, W. J., 1985. *The Design of Coupled Frame-Wall Structures for Seismic Actions*, Research Report 85-8, Dept. of Civil Engineering, University of Canterbury, Christchurch, NZ, 383p.

Goodsir W. J., Paulay, T. and Carr, A. J., 1983. A study of the inelastic seismic response of reinforced concrete coupled frame-shear wall structures, *Bulletin of the New Zealand National Society for Earthquake Engineering* **16**(3), 185-200.

Greifenhagen, C. and Lestuzzi P., 2005. Static cyclic tests on lightly reinforced concrete shear walls. *Engineering Structures*, **27**(11), 1703-1712.

Hare, H. J., Bull, D. K., Brown, B., Brunsdon, D. R., Jury, R., King, A., McCahon, I., Millar, P., Smith, P., Stannard, M. 2012. Canterbury Earthquake Sequence: Detailed Engineering Evaluation of Commercial Buildings, *Proc. of the 15 World Conf. on Earthquake Eng.*, Lisbon, Portugal.

Henry, R. S., 2013. Assessment of minimum vertical reinforcement limits for RC walls, *Bulletin of the New Zealand Society for Earthquake Engineering,* 46(2) 88-96.

Hidalgo, P. A., Ledezma, C. A., Jorden, R. M. 2002. Seismic behavior of squat reinforced concrete shear walls. *Earthquake Spectra* **18**(2), 287-308.

Hiraishi, H., 1984. Evaluation of shear and flexural deformations of flexural type shear walls, *Bulletin of the New Zealand Society for Earthquake Engineering* 17(2), 135-144.

Iliya, R. and Bertero, V. V., 1980. Effects of amounts and arrangements of wall-panel reinforcement on hysteretic behavior of reinforced concrete walls. Report UCB/EER-80/04, *Earthquake Engineering Research Center*, University of California, Berkeley.

Kam, W. Y., Pampanin, S. and Elwood, K. J., 2011. Seismic performance of reinforced concrete buildings in the 22 February Christchurch (Lyttelton) earthquake. *Bulletin of the New Zealand Society for Earthquake Engineering* **44**(4), 239-278.

Mander, J.B., Priestley, M.J.N. and Park, R., 1988. Observed stress-strain behaviour of confined concrete, *ASCE Journal of Structural Engineering* **114**(8), 1827-1849.

McVerry et al., G.H., Gerstenberger, M.C., Rhoades D.A. and Stirling M.W., 2012. Spectra and PGAs for the Assessment and Reconstruction of Christchurch. *Proc. of the New Zealand Society for Earthquake Eng. Technical Conference* NZSEE Annual Technical Conference, Christchurch.

Moehle, J.P., Ghodsi, T., Hooper, J.D., Fields, D.C., and Gedhada, R., 2011. *Seismic design of cast-in-place concrete special structural walls and coupling beams: A guide for practicing engineers*, NEHRP Seismic Design Technical Brief No. 6, National Institute of Standards and Technology, Gaithersburg, MD.

NZS 3101, 2006. Concrete Structures Standard. Wellington, New Zealand, Standards New Zealand: 646.

Paulay, T. and Priestley, M. J. N., 1992. *Seismic design of reinforced concrete and masonry buildings*. New York, John Wiley and Sons Inc.

Paulay, T. and Priestley, M. J. N., 1993. Stability of ductile structural walls", *ACI Structural Journal* **90**(4), 385-394. 744 pp.

Priestley, M. J. N., 2003. *Myths and Fallacies in Earthquake Engineering, Revisited – The Ninth Mallet Milne Lecture, 2003*, Monograph, IUSS Press, Pavia, Italy, 119 pp.

Priestley, M. J. N. and Kowalsky, M. J. 1998. Aspects of Drift and Ductility Capacity of Rectangular Cantilever Structural Walls, *Bulletin of the New Zealand Society for Earthquake Engineering,* 31(2): 73-85.

Smith, P. and England, V. 2012. Independent assessment on earthquake performance of Gallery Apartments - 62 Gloucester Street. Report prepared for the Canterbury Earthquakes Royal Commission. Retrieved from: http://canterbury.royalcommission.govt.nz/documents-by-key/20120217.3188.

Structural Engineering Society of New Zealand (SESOC), 2012. *Interim design guidance - Design of conventional structural systems following Canterbury earthquakes*, Report prepared for the Canterbury Earthquakes Royal Commission.

Wallace, J.W., Massone, L.M, Bonelli, P., Dragovich, J., Lagos, R., Lüders, C., and Moehle, J., 2012. Damage and Implications for Seismic Design of RC Structural Wall Buildings. *Earthquake Spectra* **28**(S1), S281-S299.

Wilson, A. and Lewis, C., 2011. *Novotel Cathedral Square: Structural damage report following the 22/2/11 earthquake and subsequent aftershocks*. Report prepared for the Canterbury Earthquakes Royal Commission, Christchurch, New Zealand.

Wong, P., and Vecchio, F. J., 2002. *VecTor 2 and Formworks Manual*, University of Toronto, Department of Civil Engineering, Canada.

Wood, S. L., 1989. Minimum tensile reinforcement requirements in walls, *ACI Structural Journal* **86**(5), 582-591.

Wood, S. L., Stark, R. and Greer, S. A., 1991. Collapse of eight-story RC building during 1985 Chile earthquake, *Journal of Structural Engineering* **117**(2), 600-619.

UBC, 1997. *Uniform Building Code Vol. 2*. International Conference of Building Officials.